Research Article

Power Quality Analysis Using Bilinear Time-Frequency Distributions

Abdul Rahim Abdullah[1] and Ahmad Zuri Sha'ameri[2]

[1] Faculty of Electrical Engineering, Technical university of Malaysia Malacca, 76100 Malacca, Malaysia
[2] Faculty of Electrical Engineering, Technical university of Malaysia, 81310 Johor, Malaysia

Correspondence should be addressed to Abdul Rahim Abdullah, abdulr@utem.edu.my

Bilinear time-frequency distributions (TFDs) are powerful techniques that offer good time and frequency resolution of time-frequency representation (TFR). It is very appropriate to analyze power quality signals which consist of nonstationary and multi-frequency components. However, the TFDs suffer from interference because of cross-terms. Many TFDs have been implemented, and there is no fixed window or kernel that can remove the cross-terms for all types of signals. In this paper, the bilinear TFDs are implemented to analyze power quality signals such as smooth-windowed Wigner-Ville distribution (SWWVD), Choi-Williams distribution (CWD), B-distribution (BD), and modified B-distribution (MBD). The power quality signals focused are swell, sag, interruption, harmonic, interharmonic, and transient based on IEEE Std, 1159-1995. A set of performance measures is defined and used to compare the TFRs. It shows that SWWVD presents the best performance and is selected for power quality signal analysis. Thus, an adaptive optimal kernel SWWVD is designed to determine the separable kernel automatically from the input signal.

1. Introduction

Power quality is an issue that is becoming increasingly important to electricity consumers at all levels of usage [1]. Poor power quality can cause very serious problems like reduction of lifetime of the load, the ineffective performance of protection devices, and instabilities and interruptions in manufacturing operation. For example, voltage sags to 80% of the nominal voltage with durations of 40 ms or greater would shut down the control electronics of production line of an industrial plant [2]. Thus, there is a need for heightened awareness of power quality among electricity users that require ultrahigh availability of service and precision manufacturing systems. Accordingly, an automated monitoring system is required to provide adequate coverage of the entire system, understand the causes of these disturbances, resolve existing problems, and predict future problems [1]. Prompt and accurate diagnosis of problems will ensure quality of power line signal, reduce diagnostic time in the presence of power disturbance, and rectify failures.

In the current research trend, short-time Fourier transform (STFT) [3] is a popular technique for power quality signals analysis. The technique presents the signals jointly in time-frequency representation (TFR) which provides temporal and spectral information. However, it has the limitation of a fixed window width that results is a compromise between time and frequency resolution. The greater temporal resolution required, the worse frequency resolution will be and vice versa. To overcome the limitation of the fixed resolution of STFT, wavelet transform (WT) was proposed by various researchers [4]. WT offers high time resolution for high frequency component and high frequency resolution for low frequency component. Consequently, the technique is suitable to detect the duration of high frequency signal such as transient. For low frequency signal, typically sag, swell, and interruption, it does not produce reliable results [5]. In addition, WT also exhibits some disadvantages such as its computation burden, sensitivity to noise level, and the dependency of its accuracy on the chosen basis wavelet [6].

Bilinear time-frequency distributions (TFDs) [7] have been intensively used to characterize and analyze non-stationary signals. The bilinear TFDs offer a good time and frequency resolution and are successfully applied to various real-life problems such as radar, sonar, seismic data analysis, biomedical engineering, and automatic emission. However, the TFDs suffer from the presence of cross-terms interferences because of its bilinear structure. This inhibits interpretation of its TFR, especially when signal has multiple frequency components. Some members of the bilinear TFDs are Wigner-Ville distribution (WVD), windowed Wigner-Ville distribution (WWVD), smooth-windowed Wigner-Ville distribution (SWWVD), Choi-Williams distribution (CWD), B-distribution (BD), modified B-distribution (MBD), and Born-Jordan distribution (BJD). An analysis of the autoterms presentation using the reduced interference distributions (RID) has been discussed in [8]. A procedure for designing a kernel that will produce the desired autoterm shape and an optimal kernel with respect to the autoterm quality and cross-term were demonstrated.

In this paper, bilinear TFDs are implemented to analyze power quality signals. The popular bilinear TFDs are chosen such as SWWVD, CWD, BD, and MBD. To verify the performance of the TFDs, a set of performance measures is defined to compare the TFRs in terms of main-lobe width (MLW), peak-to-side lobe ratio (PSLR), absolute percentage error (APE), and signal-to-cross-terms ratio (SCR). From the comparison, the best bilinear TFD is chosen, and its adaptive optimal kernel system is designed. The adaptive system is to determine the optimal kernel parameters, automatically from the input signal, without prior knowledge of the signal. The optimal kernel is capable of removing the cross-terms, preserving the autoterms, and maintaining accurate TFR.

2. Power Quality Signal

According to the IEEE Standards 1159, electromagnetic phenomena are classified into several groups as shown in Table 1 [9]. This paper focuses on six types of power quality signals: swell, sag, interruption, harmonic, interharmonic, and transient.

3. Signal Model

This paper divides the power quality signals into three classes. They are voltage variation for swell, sag, and interruption signal, waveform distortion for harmonic and interharmonic signal, and transient for transient signal. The signal models of the classes are formed as a complex exponential signal, and defined as

$$z_{\text{vv}}(t) = e^{j2\pi f_1 t} \sum_{k=1}^{3} A_k \Pi_k(t - t_{k-1}), \tag{1}$$

$$z_{\text{wd}}(t) = e^{j2\pi f_1 t} + A e^{j2\pi f_2 t}, \tag{2}$$

$$z_{\text{trans}}(t) = e^{j2\pi f_1 t} \sum_{k=1}^{3} \Pi_k(t - t_{k-1}) \tag{3}$$
$$+ A e^{-1.25(t-t_1)/(t_2-t_1)} e^{j2\pi f_2(t-t_1)} \Pi_2(t - t_1),$$

$$\Pi_k(t) = \begin{cases} 1, & \text{for } 0 \le t \le t_k - t_{k-1}, \\ 0, & \text{elsewhere,} \end{cases} \tag{4}$$

where $z_{\text{vv}}(t)$, $z_{\text{wd}}(t)$, and $z_{\text{trans}}(t)$ are the voltage variation, waveform distortion, and transient signal, respectively. k is the signal component sequence, A_k is the signal component amplitude, f_1 and f_2 are the signal frequency, t is the time, and $\Pi(t)$ is a box function of the signal. In this analysis, f_1, t_0, and t_3 are set at 50 Hz, 0 ms, and 200 ms, and other parameters are defined as follows:

(1) swell: $A_1 = A_3 = 1$, $A_2 = 1.2$, $t_1 = 100$ ms, $t_2 = 140$ ms,

(2) sag: $A_1 = A_3 = 1$, $A_2 = 0.8$, $t_1 = 100$ ms, $t_2 = 140$ ms,

(3) interruption: $A_1 = A_3 = 1$, $A_2 = 0$, $t_1 = 100$ ms, $t_2 = 140$ ms,

(4) harmonic: $A = 0.25$, $f_2 = 250$ Hz,

(5) interharmonic: $A = 0.25$, $f_2 = 275$ Hz,

(6) transient: $A = 0.5$, $f_2 = 1000$ Hz, $t_1 = 100$ ms, $t_2 = 115$ ms.

4. Bilinear Time-Frequency Distribution

Bilinear TFDs are powerful tools in the analysis of non-stationary and multicomponent signals. Many of these TFDs are invariant to time and frequency translations and can be considered as energy distribution in time-frequency domain [10]. From the TFR, characteristics of the signals can be calculated and used as input for signals classification. The signal characteristics are duration of swell, sag, interruption, and transient and average of total waveform distortion, total harmonic distortion, and total nonharmonic distortion. Further discussion of the signal characteristics can be found in [11].

In general, the bilinear TFDs can be formulated as

$$P_z(t, f) = \int_{-\infty}^{\infty} G(t, \tau) \underset{(t)}{*} K_z(t, \tau) \exp(-j2\pi f \tau) d\tau, \tag{5}$$

where $G(t, \tau)$ is the time-lag kernel function, $K_z(t, \tau)$ is the bilinear product, and the asterisk with t denotes the time convolution of the signals. The bilinear product is further defined as

$$K_z(t, \tau) = z\left(t + \frac{\tau}{2}\right) z^*\left(t - \frac{\tau}{2}\right), \tag{6}$$

where $z(t)$ is the analytic signal of interest. Smooth-windowed Wigner-Ville distribution (SWWVD) has a separable kernel [12] which is capable of reducing the effects of the interferences or cross-terms and at the same time, having

TABLE 1: Categories and typical characteristics of power system electromagnetic phenomena [9].

Categories	Typical spectral content	Typical duration	Typical voltage magnitude
1.0 Transients			
1.1 Impulsive			
1.1.1 Nanosecond	5 ns rise	<50 ns	
1.1.2 Microsecond	1 μs rise	50 ns–1 ms	
1.1.3 Millisecond	0.1 ms rise	>1 ms	
1.2 Oscillatory			
1.2.1 Low frequency	<5 kHz	0.3–50 ms	0–4 pu
1.2.2 Medium frequency	5–500 kHz	20 ms	0–8 pu
1.2.3 High frequency	0.5–5 MHz	5 ms	0–4 pu
2.0 Short duration variations			
2.1 Instantaneous			
2.1.1 Sag		0.5–30 cycles	0.1–0.9 pu
2.1.2 Swell		0.5–30 cycles	1.1–1.8 pu
2.2 Momentary			
2.2.1 Interruption		0.5 cycles–3s	<0.1 pu
2.2.2 Sag		30 cycles–3s	0.1–0.9 pu
2.2.3 Swell		30 cycles–3s	1.1–1.4 pu
2.3 Temporary			
2.3.1 Interruption		3 s–1 min	<0.1 pu
2.3.2 Sag		3 s–1 min	0.1–0.9 pu
2.3.3 Swell		3 s–1 min	1.1-1.2 pu
3.0 Long duration variations			
3.1 Interruption, sustained		>1 min	0.0 pu
3.2 Undervoltages		>1 min	0.8-0.9 pu
3.3 Overvoltages		>1 min	1.1-1.2 pu
4.0 Voltage imbalance		steady state	0.5–2%
5.0 Waveform distortion			
5.1 DC offset		Steady state	0–0.1%
5.2 Harmonics	0–100th H	Steady state	0–20%
5.3 Interharmonics	0–6 kHz	Steady state	0–2%
5.4 Notching		Steady state	
5.5 Noise	Broad band	Steady state	0–1%
6.0 Voltage fluctuations	<25 Hz	Intermittent	0.1–7%
7.0 Power frequency variations		<10 s	

a high time-frequency resolution. The general expression of the separable kernel is written as

$$G(t, \tau) = H(t)w(\tau), \qquad (7)$$

where $H(t)$ is the time smooth (TS) function, $w(\tau)$ is the lag window function, and its corresponding TFD can be expressed as

$$\rho_{z,\text{swwvd}}(t, f) = \int_{-\infty}^{\infty} H(t) \underset{(t)}{*} K_z(t, \tau) w(\tau) e^{-j2\pi f \tau} d\tau. \qquad (8)$$

In this paper, Hamming window is used as the lag window and raised-cosine pulse as the TS function. The hamming window and the raised-cosine pulse [12] are defined as

$$w(\tau) = \begin{cases} 0.54 + 0.46 \cos\left(\dfrac{\pi\tau}{T_g}\right), & \text{for } -T_g \leq \tau \leq T_g, \\ 0, & \text{elsewhere,} \end{cases} \qquad (9)$$

$$H(t) = \begin{cases} 1 + \cos\left(\dfrac{\pi t}{T_{\text{sm}}}\right), & \text{for } 0 \leq t \leq T_{\text{sm}}, \\ 0, & \text{elsewhere.} \end{cases} \qquad (10)$$

The lag window, $w(\tau)$, has a cutoff lag at $\tau = T_g$. The Doppler representation of the TS function, $H(t)$, that is obtained from the Fourier transform with respect to time is

$$h(v) = \frac{\sin(\pi v T_{\text{sm}})}{\pi v T_{\text{sm}}} + \frac{1}{2}\frac{\sin(\pi(v - 1/2T_{\text{sm}}))}{\pi(v - 1/2T_{\text{sm}})}$$
$$+ \frac{1}{2}\frac{\sin(\pi(v + 1/2T_{\text{sm}}))}{\pi(v + 1/2T_{\text{sm}})}, \qquad (11)$$

where it is a low-pass filter in the Doppler domain, and the cutoff Doppler frequency is

$$v_c = \frac{3}{2T_{\text{sm}}}. \qquad (12)$$

The Choi-Williams distribution (CWD) kernel is developed to reduce interference in TFDs [7] and can be defined as

$$G(t, \tau) = \frac{\sqrt{\pi\sigma}}{|\tau|}e^{-\pi^2\sigma t^2/\tau^2}, \qquad (13)$$

where σ is a real parameter that can control the resolution and the cross-terms reduction [10]. This kernel has shown good performance in reducing cross-terms while keeping high resolution with a compromise between these two requirements.

The B-distribution (BD) kernel [10] is defined in the time-lag plane and can be expressed as

$$G(t, \tau) = |\tau|^\beta \cosh^{-2\beta} t, \qquad (14)$$

where β is a positive real parameter that controls the degree of smoothing, and its value is between zero and unity. This kernel is a low-pass filter in the Doppler domain but not in the lag domain.

To improve the time resolution, the B-distribution was modified by making the lag-dependent factor exactly constant [10]. The resulting modified B-distribution (MBD) had a lag-independent kernel and can be defined as

$$G(t, \tau) = \frac{\cosh^{-2\beta} t}{\int_{-\infty}^{\infty}\cosh^{-2\beta}\xi\, d\xi}. \qquad (15)$$

5. Time-Lag Signal Characteristic

Generally, bilinear product of the signal interest is represented in time-lag representation. The bilinear product consists of autoterms and cross-terms and can be defined as

$$K_z(t, \tau) = K_{z,\text{auto}}(t, \tau) + K_{z,\text{cross}}(t, \tau). \qquad (16)$$

In the time-lag representation, normally, the autoterms are concentrated along the time axis and centered at $\tau = 0$, while the cross-terms are located away from the axis. The autoterms must be preserved, while the cross-terms are suppressed by choosing appropriate kernel parameters. For SWWVD, TS function is used to remove Doppler frequency component existing in cross-terms, while lag window suppresses cross-terms that lie away from the origin of the lag axis. Detail derivation of the autoterms and cross-terms for all signals that are shown in (17) to (32) is derived in Appendix A.
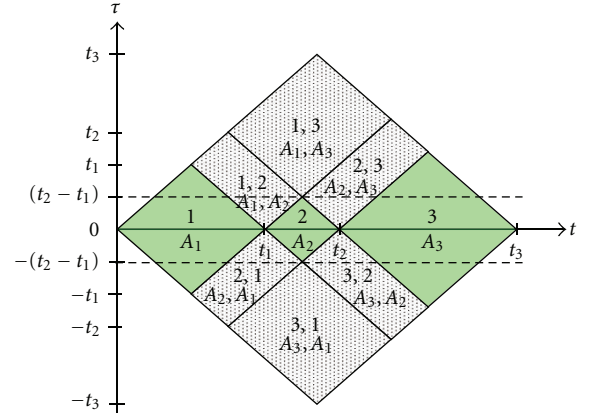

Figure 1: Bilinear product of the voltage variation signal. The autoterms are highlighted in green, while the cross-terms are densely dotted.

5.1. Bilinear Product of Voltage Variation Signal. Voltage variation signal in (1) has a variation in the root mean square (RMS) value from nominal voltage [9]. The autoterms and cross-terms of this signal can be expressed as

$$K_{\text{auto,vv}}(t, \tau) = \sum_{k=1}^{3} A_k^2 e^{j2\pi f_1 \tau} K_{\Pi_{k,k}}(t, \tau),$$

$$K_{\text{cross,vv}}(t, \tau) = \sum_{k=1}^{3}\sum_{\substack{l=1 \\ k\neq l}}^{3} A_k A_l e^{j2\pi f_1 \tau} K_{\Pi_{k,l}}(t, \tau), \qquad (17)$$

where k and l represent the signal component sequence, A_k and A_l are the signal components amplitude, and the bilinear product of the box function, $\Pi(t)$, is defined as

$$K_{\Pi_{k,l}}(t, \tau) = \Pi_k\left(t + \frac{\tau}{2} - t_k\right)\Pi_l\left(t - \frac{\tau}{2} - t_l\right). \qquad (18)$$

From (17), it is observed that the autoterms lie along the time axis and are centered at $\tau = 0$, while the cross-terms are elsewhere as shown in Figure 1.

For example, autoterm when $k = 1$ and $l = 1$ is expressed as

$$K_{\text{auto,vv}}\left(t - \frac{t_1}{2}, \tau\right) = A_1^2 e^{j2\pi f_1 \tau} K_{\Pi_{1,1}}\left(t - \frac{t_1}{2}, \tau\right). \qquad (19)$$

This autoterm is located at $t = t_1/2$ and is centered at the origin of the lag axis. It has a single lag-frequency component which is at $f = f_1$. Similar result is observed for autoterm when $k = 2$ and $l = 2$. This autoterm which is at $t = t_1/2$ is also centered at the origin of the lag axis and has a single lag-frequency component at $f = f_1$. It can be defined as

$$K_{\text{auto,vv}}\left(t - \frac{t_1 + t_2}{2}, \tau\right) = A_2^2 e^{j2\pi f_1 \tau} K_{\Pi_{2,2}}\left(t - \frac{t_1 + t_2}{2}, \tau\right). \qquad (20)$$

Meanwhile, for cross-term when $k = 1$ and $l = 2$, it is located at $t = (t_2 + 2t_1)/4$ and $\tau = t_2/2$. The cross-term is due to the interaction between 1st and 2nd signal component and has only a single lag-frequency component at $f = f_1$. It can be expressed as

$$K_{\text{cross,vv}}\left(t - \frac{t_2 + 2t_1}{4}, \tau - \frac{t_2}{2}\right)$$
$$= A_1 A_2 e^{j2\pi f_1 \tau} K_{\Pi_{1,2}}\left(t - \frac{t_2 + 2t_1}{4}, \tau - \frac{t_2}{2}\right). \tag{21}$$

Another example is cross-term which is due to the interaction between 2nd and 1st signal component. This cross-term is centered at $t = (t_2 + 2t_1)/4$ and $\tau = t_2/2$ and also has only a single lag-frequency component at $f = f_1$ as expressed in the following equation:

$$K_{\text{cross,vv}}\left(t - \frac{t_2 + 2t_1}{4}, \tau + \frac{t_2}{2}\right)$$
$$= A_1 A_2 e^{j2\pi f_1 \tau} K_{\Pi_{1,2}}\left(t - \frac{t_2 + 2t_1}{4}, \tau + \frac{t_2}{2}\right). \tag{22}$$

The examples above prove that the autoterms are centered at $\tau = 0$ and lie along the time axis, while the cross-terms are elsewhere. Since the signal has only frequency component at $f = f_1$, it results that the autoterms and cross-terms have a lag-frequency component at $f = f_1$ and zero Doppler frequency. Thus, in order to suppress the cross-terms and to preserve the autoterms, lag window should cover all autoterms while removing the cross-terms as much as possible. The lag window width, T_g, can be set as

$$\left|T_g\right| \leq t_2 - t_1. \tag{23}$$

By using this limit, cross-terms such as when $k = 1, l = 2$ and $k = 2, l = 3$ are preserved, since they are adjacent to the autoterms as shown in Figure 1. The remaining cross-terms can be reduced by using smaller T_g, but it will compromise the concentration of the autoterms. This results in smearing in frequency domain that reduces frequency resolution. In addition, the lag window width should contain at least one cycle of fundamental signal such that $T_g \geq 1/2f_1$. The actual effect of this setting will be discussed in the next section.

Since the cross-terms do not have Doppler frequency, the use of the TS function will not contribute to the cross-terms suppression. Thus, the resulting TFD that uses a lag window and an impulse function as TS function is also known as windowed Wigner-Ville distribution (WWVD). It can be expressed as

$$\rho_{z,\text{wwvd}}(t, f) = \int_{-\infty}^{\infty} K_z(t, \tau) w(\tau) e^{-j2\pi f \tau} d\tau, \tag{24}$$

where $w(\tau)$ is the lag window.

5.2. Bilinear Product of Waveform Distortion Signal.
Waveform distortion signal is a steady-state signal which consists of multiple frequency components [13]. The autoterm and cross-term of the signal in (2) can be defined as

$$K_{\text{auto,zwd}}(t, \tau) = e^{j2\pi f_1 \tau} + A^2 e^{j2\pi f_2 \tau}, \tag{25}$$

$$K_{\text{cross,zwd}}(t, \tau) = 2A e^{j2\pi((f_2 + f_1)/2)\tau} \cos(2\pi(f_2 - f_1)t). \tag{26}$$

As shown in (25), the autoterm is centered at the origin of the lag axis and has two lag-frequency components which are f_1 and f_2. For the cross-term as shown in (26), it is also centered at the origin of the lag axis. However, the cross-term consists of a lag-frequency component at $f = (f_2 + f_1)/2$ and a Doppler frequency component at $v = (f_2 - f_1)$.

Based on the observation, the Doppler frequency component only exists in the cross-term. TS function which is a low-pass filter in Doppler frequency domain can be used to remove the cross-term. Since the Doppler frequency component is at $v = (f_2 - f_1)$, the Doppler cutoff frequency should be set at $v_c \leq |f_2 - f_1|$. It can be achieved by setting the TS function parameter, T_{sm}, as

$$T_{sm} \geq \frac{3}{2|f_2 - f_1|}. \tag{27}$$

For signal that has more than two frequency components, $|f_2 - f_1|$ is set as the smallest frequency deviation among the signal frequency components. When T_{sm} is set lower than the limit in (27), the cutoff frequency will be $v_c > |f_2 - f_1|$ that will include the cross-term. Thus, the TS function will not be able to remove the cross-term. Besides that, any higher T_{sm} value would result in a small cutoff Doppler frequency but would cause the autoterm to smear in time. Thus, T_{sm} should be set at an appropriate value to remove the cross-term and avoid the smearing of autoterm in time.

Besides using the TS function to remove the cross-terms, lag window is also used to obtain desirable lag-frequency resolution in TFR. The lag-frequency resolution is set such that $\Delta f \leq f_1/2$ to differentiate harmonic and interharmonic frequency components. Therefore, the lag window width should be set at $T_g \geq 1/2\Delta f$. Higher T_g offers higher lag-frequency resolution, but it increases computation complexity and memory size to calculate TFR. Thus, T_g should be set at a sufficient value to obtain desirable lag-frequency resolution and avoid higher computation complexity and memory size used. In this analysis, since the signal fundamental frequency chosen is at $f_1 = 50$ Hz, T_g is set at minimum value which is 20 ms to reduce the computation complexity and memory size of the analysis. It results in the fact that the lag-frequency resolution of the TFR is $\Delta f = 25$ Hz. In addition, the setting is also applicable for all waveform distortion signals.

5.3. Bilinear Product of Transient Signal.
Transient signal is a sudden signal which changes in steady-state condition at nonfundamental frequency [9]. As indicated in transient signal model in (3), there are three signal components. The first and third components consist of fundamental signal,

f_1, while the second component has additional frequency component which is transient frequency, f_2. Thus, the bilinear product of this signal produces three autoterms and seven cross-terms in time-lag representation as shown in Figure 2. The autoterms and cross-terms can be expressed as

$$K_{\text{auto,trans}}(t, \tau) = e^{j2\pi f_1 \tau} K_{\Pi_{1,1}}(t, \tau)$$

$$+ \left(e^{j2\pi f_1 \tau} + A^2 e^{-2.5(t-t_1)} e^{j2\pi f_2 \tau} \right) K_{\Pi_{2,2}}(t, \tau)$$

$$+ e^{j2\pi f_1 \tau} K_{\Pi_{3,3}}(t, \tau),$$

(28)

$$K_{\text{trans,cross}}(t, \tau) = \sum_{k=1}^{3} \sum_{\substack{l=1 \\ k \neq l}}^{3} e^{j2\pi f_1 \tau} K_{\Pi_{k,l}}(t, \tau)$$

$$+ \sum_{l=1}^{3} A e^{-1.25(t+\tau/2-t_1)} e^{j2\pi(f_2-f_1)t - f_2 t_1}$$

$$\times e^{j2\pi(f_2+f_1)\tau/2} K_{\Pi_{2,l}}(t, \tau)$$

$$+ \sum_{k=1}^{3} A e^{-1.25(t+\tau/2-t_1)} e^{-j2\pi(f_2-f_1)t - f_2 t_1}$$

$$\times e^{j2\pi(f_2+f_1)\tau/2} K_{\Pi_{k,2}}(t, \tau).$$

(29)

Similar to the voltage variation signal, the autoterms in (28) are centered at $\tau = 0$ and lie along the time axis as colored in Figure 2. For example, autoterm at $k = 1$ is located at $t = t_1/2$ and the origin of the lag axis. It has a lag frequency at $f = f_1$ and can be defined as

$$K_{\text{auto,trans}}\left(t - \frac{t_1}{2}, \tau\right) = e^{j2\pi f_1 \tau} K_{\Pi_{1,1}}\left(t - \frac{t_1}{2}, \tau\right). \quad (30)$$

The location of the cross-terms in (29) is densely dotted in Figure 2. The figure shows that cross-terms that are generated by different signal components ($k \neq l$) are located away from the time axis, $\tau \neq 0$. As example, a cross-term defined in (31) is produced because of the interaction between the first and second signal components ($k = 1$ and $l = 2$). It is centered at $t = (t_2 + 2t_1)/4$ and $\tau = t_2/2$ and has a Doppler frequency component at $v = (f_2 - f_1)$ and two lag-frequency components at $f = f_1$ and $f = (f_2 + f_1)/2$:

$$K_{\text{trans,cross}}\left(t - \frac{t_2 + 2t_1}{4}, \tau - \frac{t_2}{2}\right)$$

$$= \left(e^{j2\pi f_1 \tau} + A e^{-1.25(t+\tau/2-t_1)} e^{-j2\pi(f_2-f_1)t - f_2 t_1} e^{j2\pi(f_2+f_1)\tau/2} \right)$$

$$\times K_{\Pi_{1,2}}\left(t - \frac{t_2 + 2t_1}{4}, \tau - \frac{t_2}{2}\right).$$
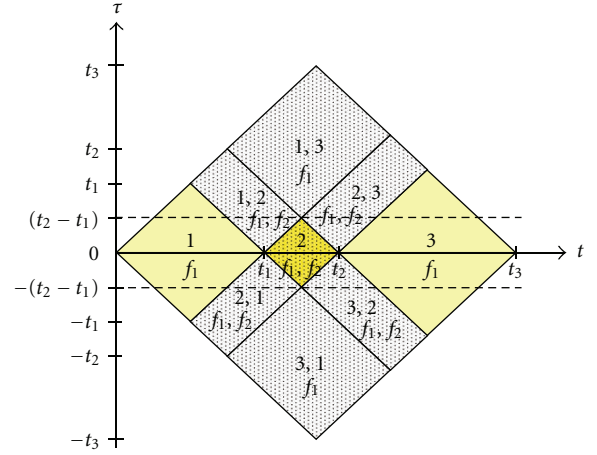
(31)

FIGURE 2: Bilinear product of the transient signal.

The second signal component has two different frequencies which are f_1 and f_2. Its bilinear product can be defined as

$$K_{z_2}(t, \tau)$$

$$= \left(e^{j2\pi f_1 \tau} + A^2 e^{-2.5(t-t_1)} e^{j2\pi f_2 \tau} + 2A e^{-1.25(t+\tau/2-t_1)} \right.$$

$$\left. \times \cos(j2\pi(f_2-f_1)t - f_2 t_1) e^{j2\pi(f_2+f_1)\tau/2} \right) K_{\Pi_{2,2}}(t, \tau).$$

(32)

This bilinear product introduces a cross-term which is located at $t = (t_2 + t_1)/2$ and also centered at $\tau = 0$, where it is similar to the autoterms. The cross-term has a Doppler frequency component at $v = (f_2 - f_1)$ and a lag frequency component at $f = (f_2 + f_1)/2$ and can be defined as

$$K_{\text{trans,cross}}\left(t - \frac{t_2 + t_1}{2}, \tau\right)$$

$$= 2A e^{-1.25(t+\tau/2-t_1)} e^{j2\pi(f_2+f_1)\tau/2} \cos(j2\pi(f_2 - f_1)t - f_2 t_1)$$

$$\times K_{\Pi_{2,2}}\left(t - \frac{t_2 + t_1}{2}, \tau\right).$$

(33)

The purpose of using lag window in this signal is similar to the voltage variation signal. The lag window width is set such that $|T_g| \leq (t_2 - t_1)$ to remove the cross-terms located away from the time axis and to preserve the autoterms lying along the time axis. In addition, similar to the waveform distortion signal, TS function is also employed to remove the Doppler frequency component of the remaining cross-terms. Since the Doppler frequency component is $v = (f_2 - f_1)$, the cutoff Doppler frequency of the TS function is set at $v_c \leq |f_2 - f_1|$ by setting the TS function parameter, T_{sm}, as in (27). An appropriate value of T_{sm} and T_g should be chosen to optimize the cross-terms suppression as well as to minimize the smearing of the autoterms in time and frequency domain.

TABLE 2: Limit of the kernel parameters.

Signal	$T_{g,min}$ (ms)	$T_{sm,min}$ (ms)
Swell	10	0
Sag	10	0
Interruption	10	0
Harmonic	20	7.5
Interharmonic	20	6.67
Transient	10	1.578

5.4. Kernel Parameters. The analysis of bilinear product in time-lag representation to determine kernel parameters for all power quality signals is discussed in the previous subsections. Based on the analysis, the limits of the kernel parameters as defined in (23) and (27) are summarized in Table 2. The smallest lag window width, $T_{g,min}$, and TS function parameter, $T_{sm,min}$, can be set in (9) and (10), respectively, to obtain sufficient cross-terms suppression with minimal autoterms bias as well as to reduce the computation complexity and memory size of the analysis.

6. Performance Comparison of Kernel Parameters

Several performance measures are created and used to verify the TFR of the bilinear TFDs. They are main-lobe width (MLW), peak-to-side lobe ratio (PSLR), signal-to-cross-terms ratio (SCR), and absolute percentage error (APE). These measurements are adopted to evaluate concentration, accuracy, interference minimization, and resolution of TFRs [12].

6.1. Performance Measurements. MLW and PSLR are calculated from the power spectrum which is obtained from the frequency marginal of the TFR [12] as shown in Figure 3. MLW is the width at 3 dB below the peak of the power spectrum, while PSLR is the power ratio between the peak and the highest side lobe calculated in dB. Low MLW indicates good frequency resolution, and it gives the ability to resolve closely spaced sinusoids. PSLR should be as high as possible to resolve signal of various magnitudes.

SCR is a ratio of signal to cross-terms power in dB. High SCR indicates high cross-terms suppression in the TFR and is defined as

$$\text{SCR} = 10 \log \left(\frac{\text{signal power}}{\text{cross} - \text{terms power}} \right). \qquad (34)$$

Besides the MLW, PSLR, and SCR, APE is also applied to quantify the accuracy of signal characteristics that are calculated from the TFR. This measurement has been discussed in [11] and is expressed as

$$\text{APE} = \frac{x_i - x_m}{x_i} \times 100\%, \qquad (35)$$

where x_i is actual value and x_m is measured value. Low APE shows high accuracy of the measurement. In general,
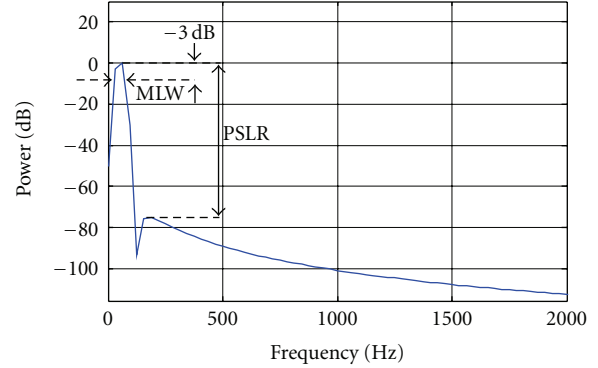

FIGURE 3: Performance measures used in the analysis.

an optimal kernel of TFD should have low MLW and APE while high PSLR and SCR.

6.2. Performance Comparison of Smooth-Windowed Wigner-Ville Distribution. The performance of SWWVD with various kernel parameters for power quality signals is shown in Table 3. In this table, the kernel parameters are chosen based on the observation made in Section 5. The bold values in Table 3 presents the parameters that give optimal TFR for each type of signal. Even though, the discussion of the table will focus on transient signal and similar observation can be made for voltage variation and waveform distortion signal.

As shown in the table, the optimal kernel parameters for the transient signal are at $T_g = 10$ ms and $T_{sm} = 1.578$ ms. To observe the performance response corresponding to the kernel parameters, the performance measures of this signal at optimal T_{sm} with various T_g and optimal T_g with various T_{sm} are plotted in Figure 4. Figure 4(a) shows that, at optimal T_{sm} and when T_g is set higher, the MLW is smaller indicating a higher frequency resolution of the TFR. However, it suffers from the reduction of the cross-terms suppression which results in smaller SCR. This is because higher T_g covers more adjacent cross-terms in lag axis in the bilinear product. As a result, the APE is higher which presents lower accuracy of the signal characteristic measurement. Since the fundamental frequency, f_1, is set at 50 Hz, the minimum T_g should be set at 10 ms to cover at least one cycle of the fundamental signal.

At the optimal T_g and when T_{sm} is set higher than its optimal value, the SCR increases, while the MLW remains constant as shown in Figure 4(b). It indicates that higher T_{sm} improves the cross-terms suppression and does not give any effect to the frequency resolution. However, the APE is also higher which shows that the time resolution of the TFR is lower. This is because the application of TS function with higher T_{sm} increases the smearing of the autoterms in time domain. Thus, there is a compromise between cross-terms suppression and time resolution to obtain optimal TFR.

The optimal kernel parameters for voltage variation signal are at $T_g = 10$ ms and $T_{sm} = 0$ ms. For this signal, the use of the TS function does not introduce any improvement in the cross-terms suppression because all cross-terms have zero

(a) MLW, APE, PSLR, and SCR at optimal T_{sm} with various T_g

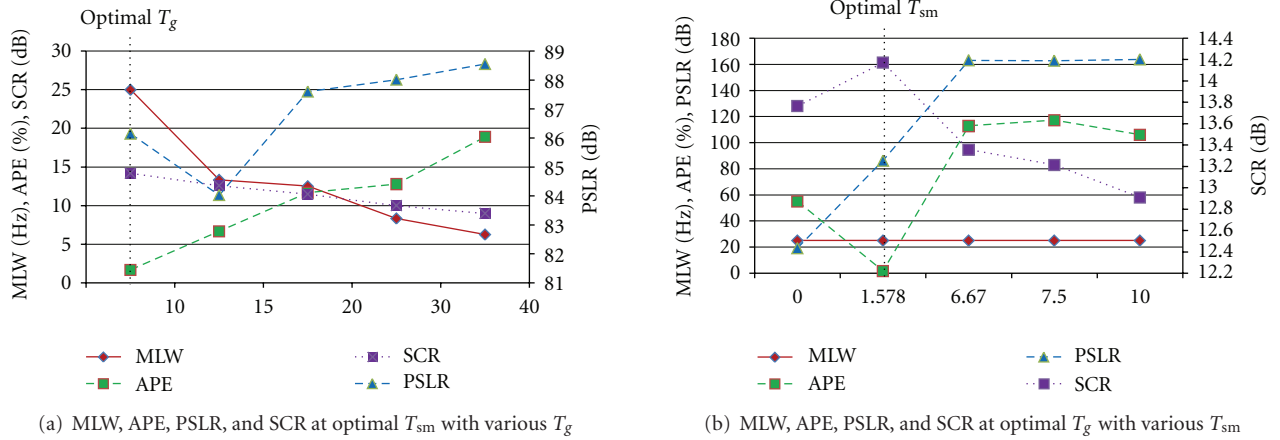(b) MLW, APE, PSLR, and SCR at optimal T_g with various T_{sm}

FIGURE 4: Performance of the TFR using SWWVD with various kernel parameters for transient signal. (The kernel parameters chosen must give low MLW and APE but high PSLR and SCR.)

TABLE 3: Performance comparison of SWWVD with various kernel parameters.

Kernel Parameters	Performance measures	Signal					
		Voltage variation signal			Waveform distortion signal		Transient signal
		Swell	Sag	Interruption	Harmonic	Interharmonic	Transient
$T_g = 10$ ms $T_{sm} = 0$ ms	MLW (Hz)	**25**	**25**	**25**	25	25	25
	PSLR (dB)	**614.82**	**614.82**	**614.82**	623.12	50.795	19.102
	SCR (dB)	**15.641**	**17.799**	**55.446**	4.4785	4.5758	13.764
	APE (%)	**0.2083**	**0.625**	**0.625**	0.3755	100	55
$T_g = 40$ ms $T_{sm} = 0$ ms	MLW (Hz)	6.25	6.25	6.25	6.25	6.25	6.25
	PSLR (dB)	117.60	117.55	89.657	644.84	652.71	86.259
	SCR (dB)	8.9462	11.216	48.903	9.0262	9.0721	9.4476
	APE (%)	1.4583	1.875	1.0417	141.27	25.031	19.444
$T_g = 10$ ms $T_{sm} = 1.578$ ms	MLW (Hz)	25	25	25	25	25	**25**
	PSLR (dB)	218.09	216.68	198.78	18.835	49.889	**86.145**
	SCR (dB)	13.491	15.038	35.107	5.6064	5.7679	**14.171**
	APE (%)	3.125	12.708	100	55.544	100	**1.6667**
$T_g = 15$ ms $T_{sm} = 1.578$ ms	MLW (Hz)	13.333	13.333	13.333	13.333	13.333	13.333
	PSLR (dB)	130.99	130.68	127.89	17.623	17.712	84.025
	SCR (dB)	11.751	13.297	33.514	10.959	11.289	12.567
	APE (%)	69.791	117.08	100	100	100	6.6667
$T_g = 20$ ms $T_{sm} = 6.67$ ms	MLW (Hz)	12.5	12.5	12.5	12.5	**12.5**	12.5
	PSLR (dB)	229.98	228.53	210.04	51.168	**638.24**	154.53
	SCR (dB)	9.8581	11.485	31.371	27.934	**23.752**	10.442
	APE (%)	14.583	29.375	100	20.142	**0.125**	107.78
$T_g = 40$ ms $T_{sm} = 6.67$ ms	MLW (Hz)	6.25	6.25	6.25	6.25	6.25	6.25
	PSLR (dB)	120.03	100.92	81.315	51.168	655.78	129.74
	SCR (dB)	6.7221	8.4121	28.701	28.570	24.256	7.7198
	APE (%)	20.416	35.417	100	20.142	0.125	90.556
$T_g = 20$ ms $T_{sm} = 7.5$ ms	MLW (Hz)	12.5	12.5	12.5	**12.5**	12.5	12.5
	PSLR (dB)	229.97	228.53	209.88	**643.28**	68.843	156.11
	SCR (dB)	9.8073	11.439	31.289	**41.007**	31.001	10.248
	APE (%)	16.666	31.667	100	**0.125**	1.4268	115
$T_g = 40$ ms $T_{sm} = 7.5$ ms	MLW (Hz)	6.25	6.25	6.25	6.25	6.25	6.25
	PSLR (dB)	122.91	102.56	111.22	664.29	651.32	131.79
	SCR (dB)	6.6568	8.3551	28.600	41.739	32.356	7.4996
	APE (%)	21.458	36.667	100	0.125	0.125	97.778

TABLE 4: Performance comparison of Choi-Williams distribution.

Kernel Parameters	Performance measures	Signal					
		Voltage variation signal			Waveform distortion signal		Transient signal
		Swell	Sag	Interruption	Harmonic	Interharmonic	Transient
$\sigma = 1.0$	MLW (Hz)	2.34375	2.34375	2.34375	2.34375	2.34375	**2.34375**
	PSLR (dB)	66.6589	66.6589	66.6589	45.5389	47.4593	**67.5132**
	SCR (dB)	5.61185	7.81444	28.6804	21.4932	22.3112	**7.0376**
	APE (%)	2.70833	3.54166	81.8750	59.5457	59.0395	**21.6667**
$\sigma = 0.5$	MLW (Hz)	2.34375	2.34375	2.34375	2.34375	2.34375	2.34375
	PSLR (dB)	78.8655	78.8655	78.8655	45.1447	47.3009	81.7881
	SCR (dB)	5.51383	7.68141	27.6884	22.9633	23.9232	6.75077
	APE (%)	1.45833	2.29166	85.2083	53.8937	55.8645	34.4444
$\sigma = 0.1$	MLW (Hz)	2.34375	2.34375	2.34375	2.34375	2.34375	2.34375
	PSLR (dB)	51.309	51.309	51.309	45.3051	52.875	51.9201
	SCR (dB)	6.0203	8.1977	27.1346	25.3153	26.4656	6.22225
	APE (%)	0.20833	0.62500	63.7500	49.3376	49.6516	49.4444
$\sigma = 0.05$	MLW (Hz)	**2.34375**	**2.34375**	**2.34375**	2.34375	2.34375	2.34375
	PSLR (dB)	**52.0779**	**52.0779**	**52.0779**	47.666	49.1118	53.6057
	SCR (dB)	**6.53223**	**8.73298**	**27.4525**	26.7083	27.7299	6.30179
	APE (%)	**0.20833**	**0.20833**	**56.8750**	44.1498	43.7457	52.2222
$\sigma = 0.01$	MLW (Hz)	5.85938	5.85938	5.85938	4.6875	4.6875	4.6875
	PSLR (dB)	57.8314	57.8314	57.8314	59.4144	61.5886	67.2973
	SCR (dB)	8.18709	10.4501	28.9207	30.6248	31.5286	7.20599
	APE (%)	0.62500	0.41666	75.0000	15.5563	28.2073	51.6667
$\sigma = 0.005$	MLW (Hz)	5.85938	5.85938	5.85938	5.85938	5.85938	5.85938
	PSLR (dB)	45.6061	45.6061	45.6061	62.4682	54.3076	57.5039
	SCR (dB)	9.03793	11.3288	29.758	30.8003	32.5905	7.8471
	APE (%)	1.04166	0.62500	78.3333	13.1708	24.7269	48.8889
$\sigma = 0.001$	MLW (Hz)	9.375	9.375	9.375	**9.375**	**9.375**	9.375
	PSLR (dB)	53.3157	53.3157	53.3157	**60.5077**	**56.1806**	58.7548
	SCR (dB)	11.2395	13.5999	32.0283	**29.0768**	**30.1635**	9.93482
	APE (%)	1.45833	1.25000	83.3333	**2.36060**	**12.7563**	49.4444

Doppler frequency. In addition, higher T_{sm} reduces the time resolution of the TFR. Therefore, as the T_{sm} is set higher, the SCR is lower, and APE is higher. For waveform distortion signal, the optimal kernel parameters for harmonic signal are at $T_g = 20$ ms and $T_{sm} = 7.5$ ms while for interharmonic signal are at $T_g = 20$ ms and $T_{sm} = 6.67$ ms. All cross-terms of these signals have Doppler frequency and can be removed by using the TS function at the optimal T_{sm}. Higher T_g does not improve the cross-terms suppression. However, it is still used to set the frequency resolution of the TFR that can differentiate between harmonic and interharmonic frequency components.

6.3. Performance Comparison of Choi-Williams Distribution.
Performance of the CWD is also compared with various kernel parameters. The kernel parameter, σ, is set at 1.0, 0.05, 0.1, 0.05, 0.01, 0.005, and 0.001 as shown in Table 4.

This table shows that the optimal parameter for voltage variation, waveform distortion, and transient signal is at $\sigma = 0.05, 0.001$, and 1.0, respectively.

All signals present similar performance response when σ is set higher or smaller than their optimal value. As example, the performance measures of sagsignal using various σ is shown graphically in Figure 5. The graph illustrates that, when σ is set higher than its optimal kernel, the MLW and SCR are smaller. Higher σ increases frequency resolution of the TFR, but it reduces cross-terms suppression. As a result, the APE is higher. As σ is set smaller, the SCR is higher because smaller σ removes more cross-terms. However, the frequency and time resolution get worse, resulting in higher MLW and APE. Thus, σ should be chosen based on the signal parameters, and a compromise between time and frequency resolution and cross-terms suppression is required to obtain optimal TFR.
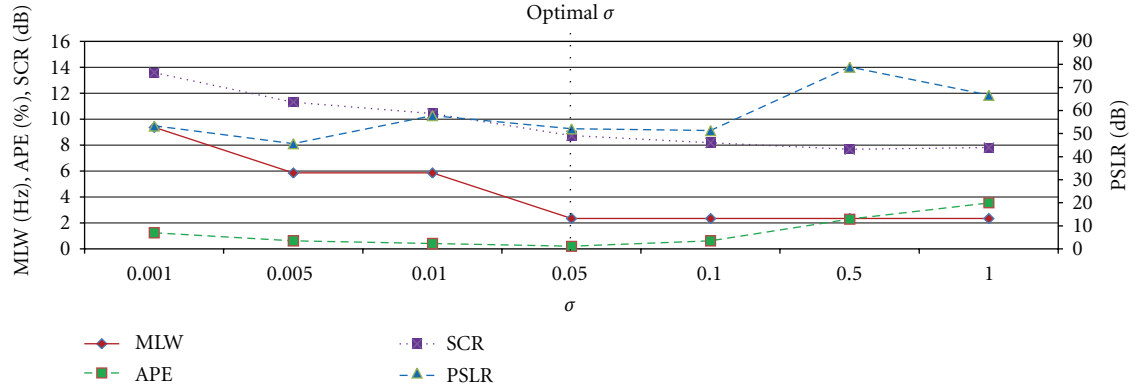
FIGURE 5: Performance comparison of the TFR using CWD with various σ for sag signal.

TABLE 5: Performance comparison of B-distribution.

Kernel parameters	Performance measures	Signal					
		Voltage variation signal			Waveform distortion signal		Transient signal
		Swell	Sag	Interruption	Harmonic	Interharmonic	Transient
$\beta = 1.0$	MLW (Hz)	2.34375	2.34375	2.34375	2.34375	2.34375	2.34375
	PSLR (dB)	17.9819	17.9819	17.9819	17.8048	17.8037	17.9819
	SCR (dB)	4.00059	6.18643	27.6292	17.8138	20.1651	6.25955
	APE (%)	26.4583	30.0000	100.000	23.5287	33.4150	100
$\beta = 0.5$	MLW (Hz)	2.34375	2.34375	2.34375	2.34375	2.34375	2.34375
	PSLR (dB)	20.4438	20.4438	20.4438	20.2938	20.2869	20.4438
	SCR (dB)	4.22834	6.38194	26.697	20.8143	24.2531	6.3561
	APE (%)	9.37500	11.8750	100.000	16.9564	21.3484	100
$\beta = 0.1$	MLW (Hz)	2.34375	2.34375	2.34375	2.34375	2.34375	2.34375
	PSLR (dB)	41.6584	41.6584	41.6584	41.3606	41.2691	41.6584
	SCR (dB)	4.75199	6.87431	26.1382	22.8579	24.2201	6.73587
	APE (%)	2.70833	3.75000	100.000	10.8960	12.3272	100
$\beta = 0.05$	MLW (Hz)	2.34375	2.34375	2.34375	**2.34375**	**2.34375**	**2.34375**
	PSLR (dB)	56.1906	56.1906	56.1906	**55.0188**	**55**	**56.1906**
	SCR (dB)	4.88367	7.00392	26.1603	**23.2079**	**24.1038**	**6.8444**
	APE (%)	2.083333	3.12500	100.000	**10.5308**	**10.1349**	**2.77778**
$\beta = 0.01$	MLW (Hz)	2.34375	2.34375	2.34375	2.34375	2.34375	2.34375
	PSLR (dB)	82.4436	82.4436	82.4436	54.1945	63.1562	82.4436
	SCR (dB)	5.0083	7.12755	26.205	19.9989	21.3782	6.94972
	APE (%)	1.66666	2.50000	100.000	15.0836	10.2403	85.5556
$\beta = 0.005$	MLW (Hz)	2.34375	2.34375	2.34375	2.34375	2.34375	2.34375
	PSLR (dB)	100	100	100	54.0775	63.0764	100
	SCR (dB)	5.04078	7.14442	26.2125	20.0266	21.1886	6.96154
	APE (%)	1.66666	2.5000	100.000	15.0483	10.2398	90
$\beta = 0.001$	MLW (Hz)	**2.34375**	**2.34375**	**2.34375**	2.34375	2.34375	2.34375
	PSLR (dB)	**100**	**100**	**100**	53.9816	63.009	100
	SCR (dB)	**5.04217**	**7.15816**	**26.2188**	20.0538	21.1648	6.9732
	APE (%)	**1.666667**	**2.50000**	**100.000**	13.4147	10.2426	92.7778

6.4. Performance Comparison of B-Distribution. BD is another TFD used in this paper. Table 5 presents the performance of the TFD with various kernel parameters, β, at 1.0, 0.05, 0.1, 0.05, 0.01, 0.005, and 0.001. The result shows that the optimal kernel for voltage variation signal is at $\beta = 0.001$ while waveform distortion and transient signal are at $\beta = 0.05$. For all signals, as β is set other than the optimal value, the MLW is similar, and the SCR is smaller. This indicates that β does not change the frequency resolution and reduce the cross-terms suppression in the TFR. As a result, the APE is higher. The trends of this performance are shown in Figure 6 which proves that the optimal kernel of harmonic is at $\beta = 0.05$.

6.5. Performance Comparison of Modified B-Distribution. MBD is also analyzed with various kernel parameters similar
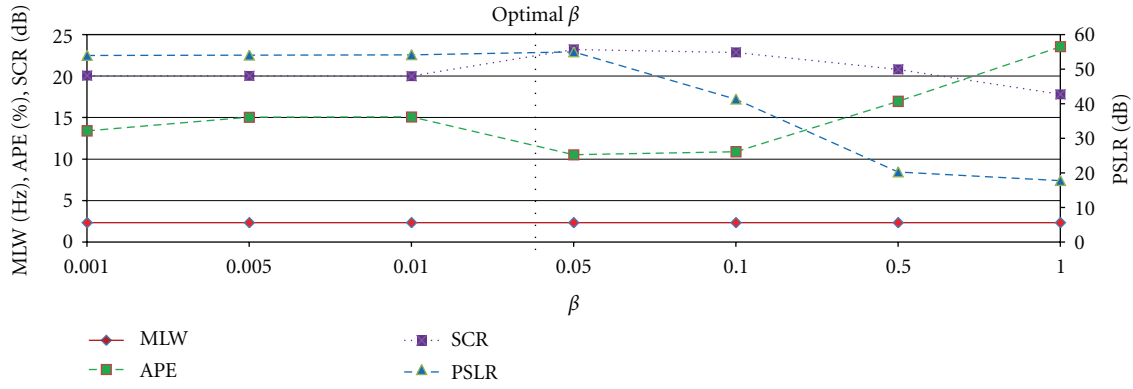
FIGURE 6: Performance comparison of the TFR using BD with various β for harmonic signal.

TABLE 6: Performance comparison of modified B-distribution.

Kernel parameters	Performance measures	Signal					
		Voltage variation signal			Waveform distortion signal		Transient signal
		Swell	Sag	Interruption	Harmonic	Interharmonic	Transient
$\beta = 1.0$	MLW (Hz)	2.34375	2.34375	**2.34375**	**2.34375**	**2.34375**	**2.34375**
	PSLR (dB)	100	100	**100**	**45.1706**	**48.2892**	**100**
	SCR (dB)	5.60786	7.88928	**29.1182**	**18.3383**	**19.6895**	**7.54363**
	APE (%)	3.54166	4.79166	**91.45833**	**12.7766**	**10.3902**	**100**
$\beta = 0.5$	MLW (Hz)	2.34375	2.34375	2.34375	2.34375	2.34375	2.34375
	PSLR (dB)	100	100	100	45.1608	48.2939	100
	SCR (dB)	5.34929	7.57329	27.7477	19.2197	20.5864	7.31436
	APE (%)	3.12500	3.95833	96.87500	24.2547	31.7169	100
$\beta = 0.1$	MLW (Hz)	2.34375	2.34375	2.34375	2.34375	2.34375	2.34375
	PSLR (dB)	100	100	100	55.1384	62.841	100
	SCR (dB)	5.09544	7.23878	26.4945	19.8685	21.1567	7.04573
	APE (%)	2.08333	2.91666	100.0000	32.3782	43.5187	100
$\beta = 0.05$	MLW (Hz)	**2.34375**	**2.34375**	2.34375	2.34375	2.34375	2.34375
	PSLR (dB)	**100**	**100**	100	54.5671	62.912	100
	SCR (dB)	**5.0679**	**7.19925**	26.3538	20.0117	21.1938	7.01054
	APE (%)	**1.66666**	**2.50000**	100.0000	34.0133	44.4557	100
$\beta = 0.01$	MLW (Hz)	2.34375	2.34375	2.34375	2.34375	2.34375	2.34375
	PSLR (dB)	100	100	100	54.0821	62.9751	100
	SCR (dB)	5.04741	7.16898	26.2465	20.0253	21.1781	6.98279
	APE (%)	1.66666	2.50000	100.0000	34.2055	44.5223	100
$\beta = 0.005$	MLW (Hz)	2.34375	2.34375	2.34375	2.34375	2.34375	2.34375
	PSLR (dB)	100	100	100	54.0199	62.9833	100
	SCR (dB)	5.04496	7.16529	26.2334	20.0315	21.1759	6.97936
	APE (%)	1.66666	2.50000	100.0000	34.2260	44.5324	100
$\beta = 0.001$	MLW (Hz)	2.34375	2.34375	2.34375	2.34375	2.34375	2.34375
	PSLR (dB)	100	100	100	53.9698	62.99	100
	SCR (dB)	5.04301	7.16236	26.223	20.0293	21.1739	6.97661
	APE (%)	1.66666	2.50000	100.0000	34.2465	44.5407	100

to BD as shown in Table 6. The table shows that the optimal kernel parameter for swell and sag is $\beta = 0.05$ while for interruption, harmonic, interharmonic, and transient signals is $\beta = 1.0$. For instance, Figure 7 shows the performance of swell signal using various β and its optimal value is identified at $\beta = 0.05$.

7. Adaptive Optimal Kernel

In the previous section, the performance of SWWVD, CWD, BD, and MBD is analyzed with various kernel parameters. From the analysis, the optimal performance of the distributions is identified and compared as shown in Table 7.
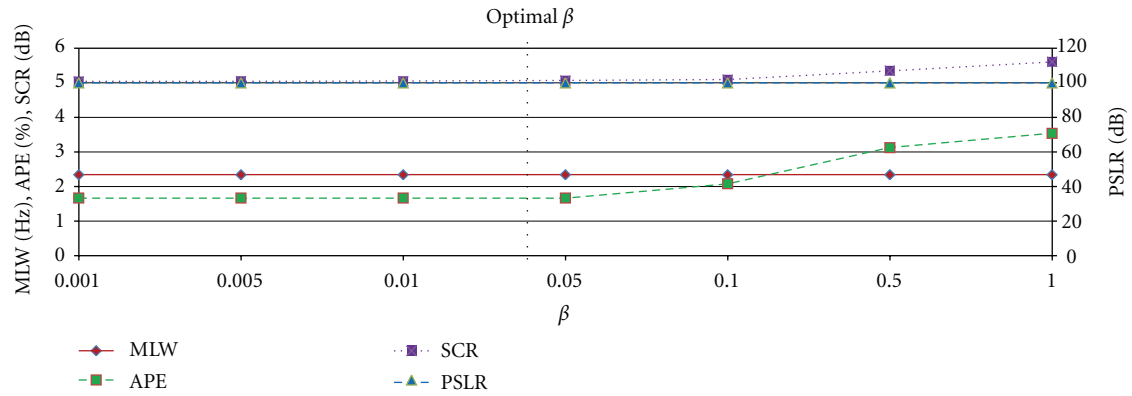
FIGURE 7: Performance comparison of the TFR using MBD with various β for swell signal.

TABLE 7: Performance comparison between optimal kernel parameters for the TFDs.

Signal			SWWVD	CWD	BD	MBD
Voltage variation signal	Swell	MLW (Hz)	**25**	2.34375	2.34375	2.34375
		PSLR (dB)	**614.815**	52.0779	100	100
		SCR (dB)	**15.6408**	6.53223	5.04217	5.0679
		APE (%)	**0.20833**	0.20833	1.66666	1.66666
	Kernel parameter		$T_g = \mathbf{10\ ms}$ $T_{sm} = \mathbf{0\ ms}$	$\sigma = 0.05$	$\beta = 0.001$	$\beta = 0.05$
	Sag	MLW (Hz)	**25**	2.34375	2.34375	2.34375
		PSLR (dB)	**614.815**	52.0779	100	100
		SCR (dB)	**17.7996**	8.73298	7.15816	7.19925
		APE (%)	**0.625**	0.20833	2.50000	2.50000
	Kernel parameter		$T_g = \mathbf{10\ ms}$ $T_{sm} = \mathbf{0\ ms}$	$\sigma = 0.05$	$\beta = 0.001$	$\beta = 0.05$
	Interruption	MLW (Hz)	**25**	2.34375	2.34375	2.34375
		PSLR (dB)	**614.815**	52.0779	100	100
		SCR (dB)	**55.4463**	27.4525	26.2188	29.1182
		APE (%)	**0.625**	56.8750	100.000	91.458
	Kernel parameter		$T_g = \mathbf{10\ ms}$ $T_{sm} = \mathbf{0\ ms}$	$\sigma = 0.05$	$\beta = 0.001$	$\beta = 1.0$
Waveform distortion signal	Harmonic	MLW (Hz)	**6.25**	9.375	2.34375	2.34375
		PSLR (dB)	**664.295**	60.5077	55.0188	45.1706
		SCR (dB)	**41.7393**	29.0768	23.2079	18.3383
		APE (%)	**0.125**	2.36060	10.5308	12.7766
	Kernel parameter		$T_g = \mathbf{20\ ms}$ $T_{sm} = \mathbf{7.5\ ms}$	$\sigma = 0.001$	$\beta = 0.05$	$\beta = 1.0$
	Interharmonic	MLW (Hz)	**6.25**	9.375	2.34375	2.34375
		PSLR (dB)	**655.776**	56.1806	55	48.2892
		SCR (dB)	**42.256**	30.1635	24.1038	19.6895
		APE (%)	**0.125**	25.5125	10.1349	10.3902
	Kernel parameter		$T_g = \mathbf{20\ ms}$ $T_{sm} = \mathbf{6.67\ ms}$	$\sigma = 0.001$	$\beta = 0.05$	$\beta = 1.0$
Transient signal	Transient	MLW (Hz)	**25**	2.34375	2.34375	2.34375
		PSLR (dB)	**86.1447**	67.5132	56.1906	56.1906
		SCR (dB)	**14.1705**	7.0376	6.8444	6.8444
		APE (%)	**1.66667**	21.6667	2.77778	2.77778
	Kernel parameter		$\mathbf{T_g = 10\ ms}$ $\mathbf{T_{sm} = 1.58\ ms}$	$\sigma = 1.0$	$\beta = 0.05$	$\beta = 1.0$

The result shows that the SWWVD is the best distribution for power quality signal analysis and an adaptive optimal kernel for SWWVD is designed.

Based on the analysis in Sections 5 and 6, a guideline to determine the separable kernel parameters of SWWVD for power quality signals is given as follows.

(i) For voltage variation signal

$$T_g = 10\,\text{ms}, \qquad T_{\text{sm}} = 0\,\text{ms}. \tag{36}$$

(ii) For waveform distortion signal

$$T_g = 20\,\text{ms}, \qquad T_{\text{sm}} = \frac{3}{2\,|f_2 - f_1|}. \tag{37}$$

(iii) For transient

$$T_g = 10\,\text{ms}, \qquad T_{\text{sm}} = \frac{3}{2\,|f_2 - f_1|}. \tag{38}$$

The kernel parameters are different based on the characteristics of the signals. Hence, an adaptive kernel system is required which is capable of setting the kernel parameters automatically from input signal. In this paper, based on the kernels setting given above, the adaptive kernel system for power quality signal is designed as shown in Figure 8.

Firstly, bilinear product at $\tau = 0$ for the input signal is calculated. It can also be called instantaneous energy of the interest signal, $x(t)$ [14], and can be expressed as

$$K_x(t, 0) = x(t)x^*(t). \tag{39}$$

For the signal models in (1) to (3), the bilinear product at $\tau = 0$ of the voltage variation, waveform distortion, and transient signal are, respectively, defined as

$$K_{z,\text{vv}}(t, 0) = \sum_{k=1}^{3} A_k^2 \Pi_k(t - t_k),$$

$$K_{z,\text{wd}}(t, 0) = 1 + A^2 + 2A\cos(2\pi(f_2 - f_1)t),$$

$$K_{z,\text{trans}}(t, 0) = \sum_{k=1}^{3} \Pi_k(t - t_k)$$

$$+ \left(A^2 e^{-2.5(t-t_1)} + 2A e^{-1.25(t+\tau/2-t_1)}\right.$$

$$\left. \times \cos(j2\pi(f_2 - f_1)t - f_2 t_1)\right)\Pi_2(t - t_2). \tag{40}$$

The above equations show that the voltage variation and transient signal have a momentary energy variation between t_1 and t_2, while the waveform distortion has no momentary energy variation. Thus, based on this observation and the guideline given in (36) to (38), the lag window width is set at $T_g = 10\,\text{ms}$ for the signal that has momentary energy variation, while, for no momentary energy variation, T_g is set at 20 ms.

In process to estimate TS function parameters, T_{sm}, ambiguity function of the bilinear at $\tau = 0$ is employed.

Power quality signal

→

Calculate bilinear product at $\tau = 0$

Calculate ambiguity function at $\tau = 0$ | Identify magnitude pattern

Estimate time-smooth function parameter | Estimate lag window width

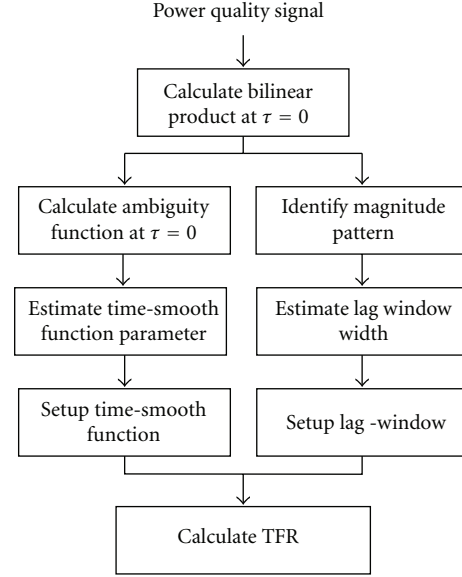Setup time-smooth function | Setup lag -window

Calculate TFR

FIGURE 8: Process flow of the adaptive optimal SWWVD.

It is calculated by using (41) to present the Doppler frequency component of the bilinear product. From the ambiguity function, the lowest Doppler frequency, v_{min}, is identified and used to calculate T_{sm} as defined in (42):

$$A_z(v, 0) = \int_{-\infty}^{\infty} K_z(t, 0)e^{-j2\pi vt} dt, \tag{41}$$

$$T_{\text{sm}} = \left[\frac{3}{2v_{\text{min}}}\right]. \tag{42}$$

As indicated in (40), the waveform distortion and transient signal have a Doppler frequency component at $v = |f_2 - f_1|$ while the voltage variation has zero Doppler frequency. Thus, for waveform distortion and transient signal, v_{min} is set at $|f_2 - f_1|$ and is then used in (42) to calculate T_{sm}. Since the voltage variation has no Doppler frequency, the time-smooth function parameter is set at $T_{\text{sm}} = 0\,\text{ms}$, or, in other words, the TS function used is a delta function. For normal signal, it has zero Doppler frequency as well as no energy variation. Therefore, the kernel parameters used are similar to the voltage variation signal which are $T_g = 10\,\text{ms}$ and $T_{\text{sm}} = 0\,\text{ms}$. Finally, the setting of the kernels is used to calculate the SWWVD to represent the signal in TFR.

For example, Figures 9 to 11 show swell, harmonic, and transient signals and their bilinear product and ambiguity function at $\tau = 0$, respectively. As shown in Figure 9(a), the magnitude of the swell signal is 1.2 pu starting from 100 to 140 ms, while Figure 9(b) shows that its energy increases from 1 to 1.44 pu between 100 and 140 ms. The signal has zero Doppler-frequency as shown in Figure 9(c). For harmonic signal in Figure 10(a), it is a constant sinusoidal energy as shown in Figure 10(b), while Figure 10(c) shows its Doppler frequency is $v = 200\,\text{Hz}$. It is different from the transient signal that has a short energy variation between 100 and 115 ms, while its Doppler frequency is at $v = 950\,\text{Hz}$ as shown in Figures 11(b) and 11(c), respectively.

FIGURE 9: (a) Swell signal, (b) its bilinear product, and (c) ambiguity function at $\tau = 0$.
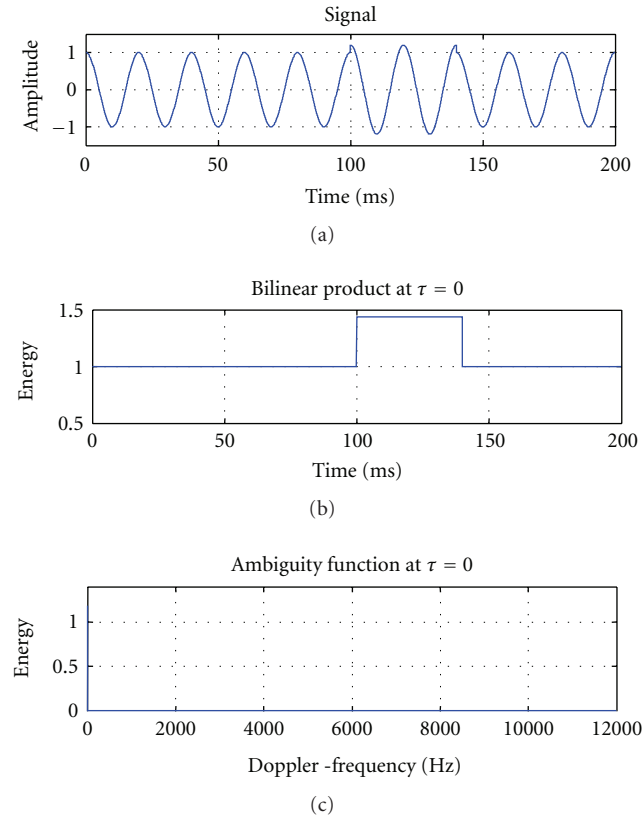

FIGURE 10: (a) Harmonic signal, (b) its bilinear product, and (c) ambiguity function at $\tau = 0$.

Based on the adaptive system design, since the bilinear product at $\tau = 0$ of swell and transient signals has a momentary energy variation, the lag window width is set at $T_g = 10$ ms. For harmonic signal that has no momentary energy variation, the lag window width is set at $T_g = 20$ ms. The harmonic and transient signals have a Doppler frequency. Thus, the values of the Doppler frequency are used in (42) to calculate T_{sm}. As a result, the setting of T_{sm} for the harmonic and transient signals is 7.5 and 1.578 ms, respectively. For the swell signal, it has no Doppler frequency component, and T_{sm} is set at 0 ms.

8. Results

In this section, the results of the power quality analysis using SWWVD, CWD, BD, and MBD are discussed. The example of the signals and their TFRs using the TFDs at optimal kernels is shown in Figures 12 to 15. The line graphs show the signal in time domain, while the contour plots show the TFR. The highest power is represented in red color while the lowest in blue color.

Figure 12 shows a sag signal and its TFR using SWWVD. The magnitude of the sag signal is 0.8 pu, while its duration is between 100 and 140 ms. The contour plot presents that there is a momentary decrease of power at 50 Hz (fundamental frequency) from 100 to 140 ms. In Figure 13, there is a harmonic signal in time domain and its TFR
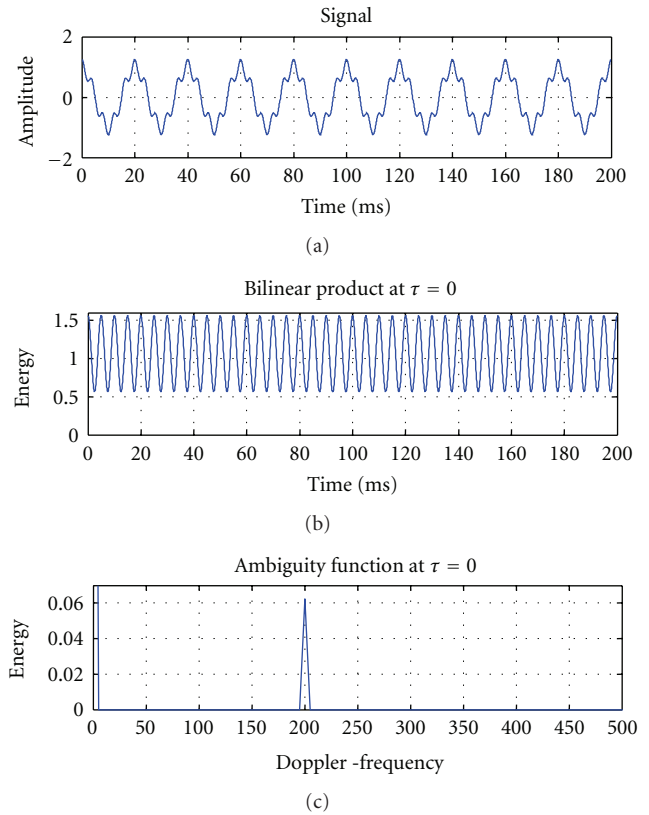
by using CWD. The TFR shows that the harmonic signal consists of two frequency components which are 50 and 250 Hz.

A swell signal and its TFR using BD are shown in Figure 14. The magnitude of the swell signal is 1.2 pu between 100 and 140 ms. The TFR shows that the power increases from 120 to 160 ms, and its frequency is 50 Hz. The last example is transient signal. This signal and its TFR using MBD are shown in Figure 15. The transient signal begins at 100 ms, and its duration is 15 ms. In the contour plot, the transient power increases between 118 and 125 ms, and its frequency is 1000 Hz.

In the contour plots, the TFRs show some delays compared to the input signals. This is because the convolution process between kernel and signal in the TFDs shifts the TFRs in time domain. For the TFR of sag signal using SWWVD, there is no delay because the kernel parameter used for time-smooth function is set at $T_{sm} = 0$ ms. Generally, this observation clearly shows that the TFRs represent the characteristics of the power quality signals.

By assuming perfect knowledge of the power quality signals, the performance of the bilinear TFDs with various kernel parameters has been analyzed as shown in Tables 3 to 6. From those tables, the optimal performance of the TFDs is identified and summarized in Table 7.

A good TFD should have low APE and MLW while high SCR and PSLR. This table shows that, in overall, SWWVD
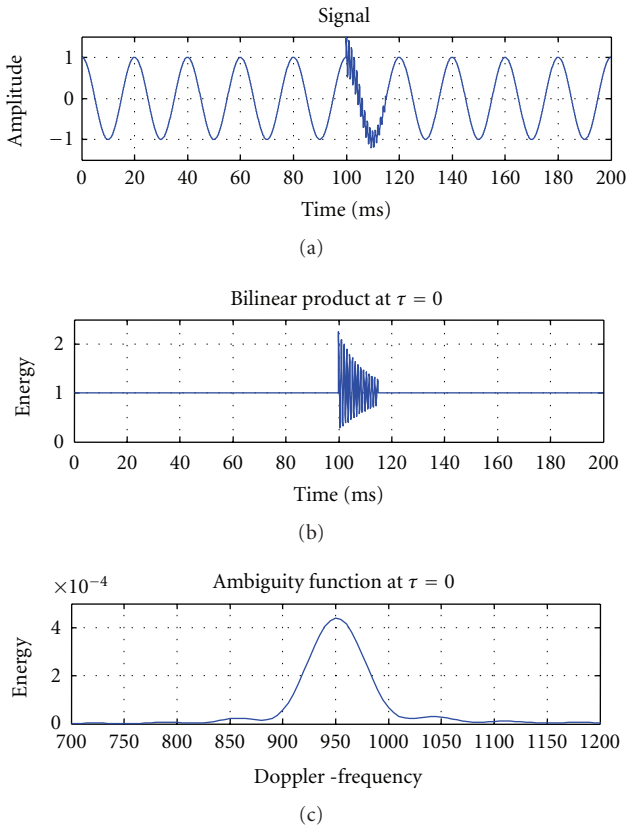
FIGURE 11: (a) Harmonic signal, (b) its bilinear product, and (c) ambiguity function at $\tau = 0$.
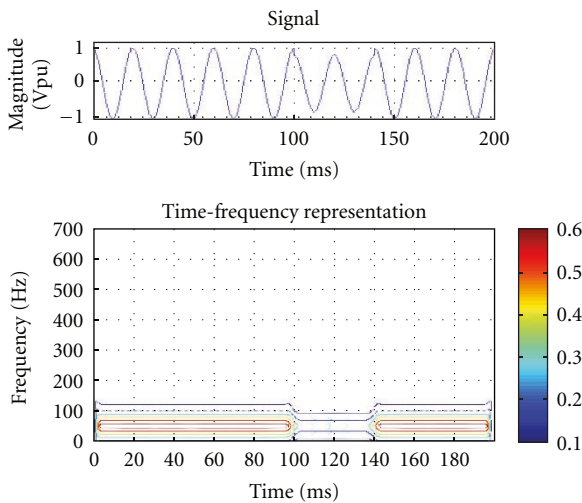

FIGURE 12: The TFR of sag signal using SWWVD at $T_g = 10$ ms and $T_{sm} = 0$ ms.

gives good APE, SCR, and PSLR while MLW is poor. For CWD, BD, and MBD, they offer good MLW but poor APE, SCR, and PSLR. Thus, it clearly proves that the SWWVD is the best distribution and very appropriate for power quality analysis.
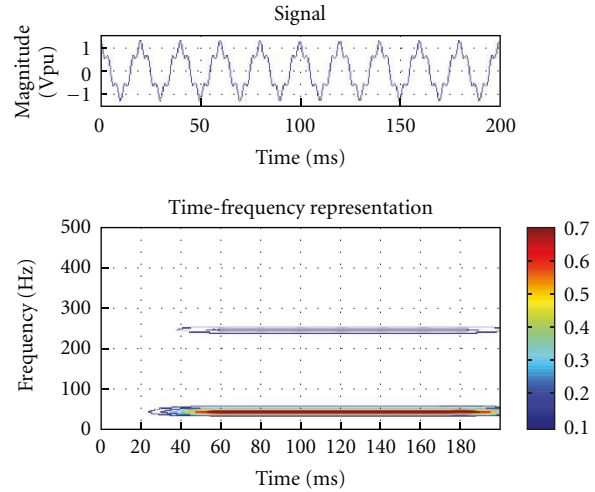
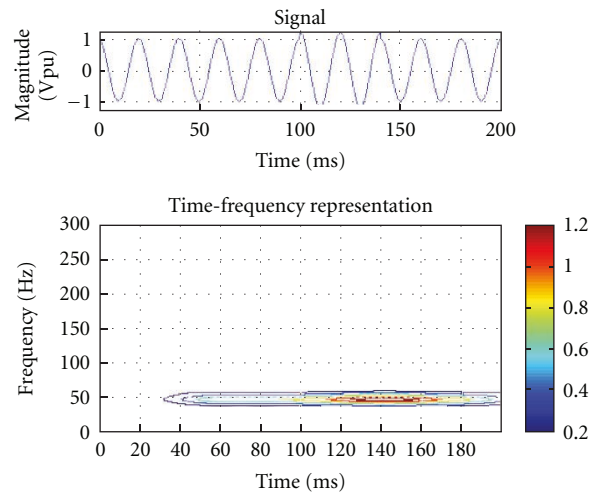

FIGURE 13: The TFR of harmonic signal using CWD at $\sigma = 0.001$.

FIGURE 14: The TFR of swell signal using BD at $\beta = 0.001$.
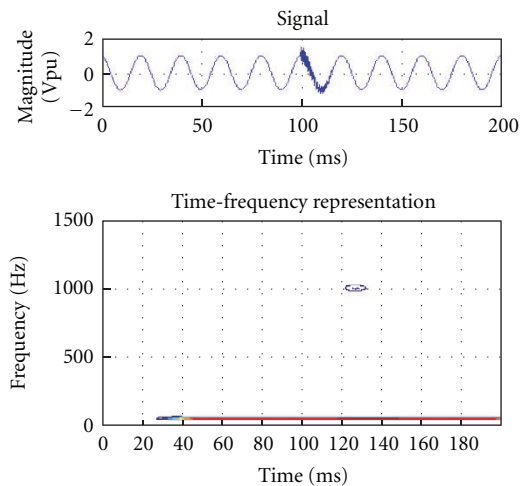

FIGURE 15: The TFR of transient signal using MBD at $\beta = 1.0$.

TABLE 8: Performance comparison between optimal and adaptive optimal kernel parameters.

Signal		Performance measures	Optimal	Adaptive
Voltage variation signal	Swell	MLW (Hz)	25	25
		PSLR (dB)	614.815	614.815
		SCR (dB)	15.6408	15.6408
		APE (%)	0.20833	0.20833
	Sag	MLW (Hz)	25	25
		PSLR (dB)	614.815	614.815
		SCR (dB)	17.7996	17.7996
		APE (%)	0.625	0.625
	Interruption	MLW (Hz)	25	25
		PSLR (dB)	614.815	614.815
		SCR (dB)	55.4463	55.4463
		APE (%)	0.625	0.625
	Kernel parameter	T_g (ms)	10	10
		T_{sm} (ms)	0	0
Waveform distortion signal	Harmonic	MLW (Hz)	6.25	6.25
		PSLR (dB)	664.295	664.295
		SCR (dB)	41.7393	41.7393
		APE (%)	0.125	0.125
	Kernel parameter	T_g (ms)	20	20
		T_{sm} (ms)	7.5	7.5
	Interharmonic	MLW (Hz)	6.25	6.25
		PSLR (dB)	655.776	655.776
		SCR (dB)	42.256	42.256
		APE (%)	0.125	0.125
	Kernel parameter	T_g (ms)	20	20
		T_{sm} (ms)	6.67	6.67
Transient signal	Transient	MLW (Hz)	25	25
		PSLR (dB)	86.1447	86.1447
		SCR (dB)	14.1705	14.1705
		APE (%)	1.66667	1.66667
	Kernel parameter	T_g (ms)	10	10
		T_{sm} (ms)	1.578	1.578

For any unknown signal, an adaptive optimal kernel SWWVD system is designed as discussed in Section 7 to determine automatically the optimal kernel parameters. Then, the performance of the adaptive kernel is identified and compared with the performance of the optimal kernel as shown in Table 8.

This table shows that, for every signal, the adaptive kernel gives similar parameters to the optimal kernel. As a result, the performance of adaptive kernel is comparable to the performance of optimal kernel. In addition, the adaptive system also gives high accuracy for the measurement of the signal characteristics as discussed in Section 6.1. Therefore, the adaptive kernel system is suitable to be implemented for power quality analysis as well as for classification purpose.

The performance of SWWVD for power quality signals classification in noisy condition has been discussed in [15]. A set of 100 signals with various characteristics for each type of power quality signal were generated and classified at SNR from 0 to 40 dB. The results show that the system can classify all signals without error at 36 dB of SNR and above.

9. Conclusions

This paper presents the analysis of power quality signals using SWWVD, CWD, BD, and MBD to identify the optimal kernel parameters. The performance measures used are MLW, PSLR, SCR, and APE. The results show that different power quality signals need different kernel parameters for optimal TFR. There is no one kernel parameter that can be used optimally for all signals.

At the optimal kernel setting, the SWWVD gives the best performance of TFR compared to the other TFDs, and its adaptive optimal kernel is designed. The adaptive system can obtain optimal kernel setting automatically without prior knowledge of the signal. The result shows that the adaptive kernels system is comparable to the optimal kernel and is suitable for power quality analysis and classification purpose.

Appendices

The bilinear product that is given in (6) represents a signal in time-lag representation. This representation consists of two terms: autoterms and cross-terms as defined in (16). This section discusses the calculation of bilinear product to obtain the autoterms and cross-terms for the power quality signals.

A. The Voltage Variation Signal

The voltage variation signal in (1) has three sequence signals at fundamental frequency, f_1, and its bilinear product is given as

$$
\begin{aligned}
K_{z,\mathrm{vv}}(t,\tau) &= \left(e^{j2\pi f_1(t+\tau/2)} \sum_{k=1}^{3} A_k \Pi_k \left(t + \frac{\tau}{2} - t_{k-1} \right) \right) \\
&\quad \times \left(e^{-j2\pi f_1(t-\tau/2)} \sum_{l=1}^{3} A_l \Pi_l \left(t - \frac{\tau}{2} - t_{l-1} \right) \right) \\
&= e^{j2\pi f_1 \tau} \sum_{k=1}^{3} \sum_{l=1}^{3} A_k A_l \Pi_k \left(t + \frac{\tau}{2} - t_{k-1} \right) \\
&\quad \times \Pi_l \left(t - \frac{\tau}{2} - t_{l-1} \right),
\end{aligned}
$$

(A.1)

where A_k and A_l are the signal amplitude, t_k and t_l are the time, k and l are the signal sequence starting with one, and $\Pi(t)$ is a box function of the signal as expressed in (4).

The autoterms are bilinear product of a signal with the same signal, $k = l$. Thus, the autoterms for this signal are defined as

$$
\begin{aligned}
K_{\text{auto,vv}}(t,\tau) &= e^{j2\pi f_1 \tau} \sum_{k=1}^{3} |A_k|^2 \Pi_k\left(t + \frac{\tau}{2} - t_{k-1}\right) \\
&\quad \times \Pi_k\left(t - \frac{\tau}{2} - t_{k-1}\right) \\
&= e^{j2\pi f_1 \tau} \sum_{k=1}^{3} |A_k|^2 K_{\Pi_{k,k}}(t,\tau),
\end{aligned} \tag{A.2}
$$

$$
K_{\Pi_{k,l}}(t,\tau) = \Pi_k\left(t + \frac{\tau}{2} - t_{k-1}\right) \Pi_l\left(t - \frac{\tau}{2} - t_{k-1}\right).
$$

The cross-terms are bilinear product between different signal, $k \neq l$, and expressed as

$$
\begin{aligned}
K_{\text{cross,vv}}(t,\tau) &= e^{j2\pi f_1 \tau} \sum_{k=1}^{3} \sum_{\substack{l=1 \\ k \neq l}}^{3} A_k A_l \Pi_k\left(t + \frac{\tau}{2} - t_{k-1}\right) \\
&\quad \times \Pi_l\left(t - \frac{\tau}{2} - t_{l-1}\right) \\
&= e^{j2\pi f_1 \tau} \sum_{k=1}^{3} \sum_{\substack{l=1 \\ k \neq l}}^{3} A_k A_l K_{\Pi_{k,l}}(t,\tau).
\end{aligned} \tag{A.3}
$$

B. The Waveform Distortion Signal

The waveform distortion signal in (2) is different from the previous signal that has one signal and consists of two frequency components, f_1 and f_2. Its bilinear product is expressed as

$$
\begin{aligned}
K_{z,\text{wd}}(t,\tau) &= \left(e^{j2\pi f_1(t+\tau/2)} + A e^{j2\pi f_2(t+\tau/2)}\right) \\
&\quad \times \left(e^{-j2\pi f_1(t-\tau/2)} + A e^{-j2\pi f_2(t-\tau/2)}\right) \\
&= e^{j2\pi f_1 \tau} + A^2 e^{j2\pi f_2 \tau} + 2A e^{j2\pi((f_2+f_1)/2)\tau} \\
&\quad \times \cos(2\pi(f_2 - f_1)t).
\end{aligned} \tag{B.1}
$$

The function above shows that the autoterms have two lag-frequency components similar to the signal frequencies, f_1 and f_2 frequencies, while the cross-terms exist in the middle between the lag-frequency components, $(f_2 + f_1)/2$, and have a Doppler frequency at $v = f_2 - f_1$. The autoterms and cross-terms are defined as

$$
K_{\text{auto,zwd}}(t,\tau) = e^{j2\pi f_1 \tau} + A^2 e^{j2\pi f_2 \tau},
$$
$$
K_{\text{cross,zwd}}(t,\tau) = 2A e^{j2\pi((f_2+f_1)/2)\tau} \cos(2\pi(f_2 - f_1)t). \tag{B.2}
$$

C. The Transient Signal

The transient signal in (3) has three sequence signals. The first and third signals are normal signal at fundamental frequency, f_1, while the second signal has additional transient frequency, f_2. The bilinear product of this signal is defined as

$$
\begin{aligned}
K_{z,\text{trans}}(t,\tau) &= \left(e^{j2\pi f_1(t+\tau/2)} \sum_{k=1}^{3} \Pi_k\left(t + \frac{\tau}{2} - t_{k-1}\right)\right. \\
&\quad + A e^{-1.25(t+\tau/2-t_1)/t_d} e^{j2\pi f_2(t+\tau/2-t_1)} \\
&\quad \left. \times \Pi_2\left(t + \frac{\tau}{2} - t_1\right)\right) \\
&\quad \times \left(e^{-j2\pi f_1(t-\tau/2)} \sum_{l=1}^{3} \Pi_l\left(t - \frac{\tau}{2} - t_{k-1}\right)\right. \\
&\quad + A e^{-1.25(t-\tau/2-t_1)/t_d} e^{-j2\pi f_2(t-\tau/2-t_1)} \\
&\quad \left. \times \Pi_2\left(t - \frac{\tau}{2} - t_1\right)\right) \\
&= A^2 e^{-2.5(t-t_1)} e^{j2\pi f_2 \tau} K_{\Pi_{2,2}}(t,\tau) \\
&\quad + \sum_{k=1}^{3} \sum_{l=1}^{3} e^{j2\pi f_1 \tau} K_{\Pi_{k,l}}(t,\tau) \\
&\quad + \sum_{l=1}^{3} A e^{-1.25(t+\tau/2-t_1)} e^{-j2\pi(f_2-f_1)t-f_2 t_1} \\
&\quad \times e^{j2\pi(f_2+f_1)\tau/2} K_{\Pi_{2,l}}(t,\tau) \\
&\quad + \sum_{k=1}^{3} A e^{-1.25(t+\tau/2-t_1)} e^{-j2\pi(f_2-f_1)t-f_2 t_1} \\
&\quad \times e^{j2\pi(f_2+f_1)\tau/2} K_{\Pi_{k,2}}(t,\tau).
\end{aligned} \tag{C.1}
$$

As discussed for the voltage variation and waveform distortion signal, autoterms and cross-terms of transient signal can be defined as

$$
\begin{aligned}
K_{\text{auto,trans}}(t,\tau) &= \sum_{k=1}^{3} e^{j2\pi f_1 \tau} K_{\Pi_{k,k}}(t,\tau) + A^2 e^{-2.5(t-t_1)} e^{j2\pi f_2 \tau} \\
&\quad \times K_{\Pi_{2,2}}(t,\tau),
\end{aligned}
$$

$$
\begin{aligned}
K_{\text{trans,cross}}(t,\tau) &= \sum_{k=1}^{3} \sum_{l=1}^{3} e^{j2\pi f_1 \tau} K_{\Pi_{k,l}}(t,\tau) \\
&\quad + \sum_{l=1}^{3} A e^{-1.25(t+\tau/2-t_1)} e^{j2\pi(f_2-f_1)t-f_2 t_1} \\
&\quad \times e^{j2\pi(f_2+f_1)\tau/2} K_{\Pi_{2,l}}(t,\tau) \\
&\quad + \sum_{k=1}^{3} A e^{-1.25(t+\tau/2-t_1)} e^{-j2\pi(f_2-f_1)t-f_2 t_1} \\
&\quad \times e^{j2\pi(f_2+f_1)\tau/2} K_{\Pi_{k,2}}(t,\tau).
\end{aligned} \tag{C.2}
$$

Acknowledgments

References

[1] D. B. Vannoy, M. F. McGranaghan, S. M. Halpin, W. A. Moncrief, and D. D. Sabin, "Roadmap for power-quality standards development," *IEEE Transactions on Industry Applications*, vol. 43, no. 2, pp. 412–421, 2007.

[2] R. B. Godoy, J. O. P. Pinto, and L. Galotto Jr., "Multiple signal processing techniques based power quality disturbance detection, classification, and diagnostic software," in *Proceedings of the 9th International Conference on Electrical Power Quality and Utilisation (EPQU '07)*, pp. 1–6, Barcelona, Spain, October 2007.

[3] K.-K. Poh and P. Marziliano, "Analysis of neonatal EEG signals using stockwell transform," in *Proceedings of the IEEE International Conference on Engineering in Medicine and Biology Society (EMBS '07)*, pp. 594–597, Lyon, France, August 2007.

[4] Z. Shi, L. Ruirui, W. Qun, J. T. Heptol, and Y. Guimin, "The research of power quality analysis based on improved S-transform," in *Proceedings of the 9th International Conference on Electronic Measurement and Instruments (ICEMI '09)*, vol. 2, pp. 2477–2481, Beijing, China, August 2009.

[5] T. Radii, P. M. Ramos, and A. C. Serra, "Detection and extraction of harmonic and non-harmonic power quality disturbances using sine fitting methods," in *Proceedings of the 13th International Conference on Harmonics and Quality of Power (ICHQP '08)*, pp. 1–6, Wollongong, Australia, September 2008.

[6] F. Zhao and R. Yang, "Power-quality disturbance recognition using S-transform," *IEEE Transactions on Power Delivery*, vol. 22, no. 2, pp. 944–950, 2007.

[7] B. Barkat and B. Boashash, "A high-resolution quadratic time-frequency distribution for multicomponent signals analysis," *IEEE Transactions on Signal Processing*, vol. 49, no. 10, pp. 2232–2239, 2001.

[8] L. Stanković, "Auto-term representation by the reduced interference distributions: a procedure for kernel design," *IEEE Transactions on Signal Processing*, vol. 44, no. 6, pp. 1557–1563, 1996.

[9] "IEEE recommended practice for monitoring electrical power quality," IEEE Standards 1159-1995 Approved, June 1995.

[10] B. Boashash, *Time-Frequency Signal Analysis and Processing: A Comprehensive Reference*, Elsevier, Amsterdam, The Netherlands, 2003.

[11] A. R. Abdullah and A. Z. Sha'ameri, "Power quality analysis using linear time-frequency distribution," in *Proceedings of the 2nd IEEE International Power and Energy Conference (PECon '08)*, pp. 313–317, Johor, Malaysia, December 2008.

[12] J. L. Tan and A. Z. B. Sha'Ameri, "Adaptive optimal kernel smooth-windowed wigner-ville distribution for digital communication signal," *EURASIP Journal on Advances in Signal Processing*, vol. 2008, Article ID 408341, 2008.

[13] A. Moreno, *Power Quality: Mitigation Technologies in a Distributed Environment*, Springer, New York, NY, USA, 2007.

[14] Z. Sharif, M. S. Zainal, A. Z. Sha'ameri, and S. H. S. Salleh, "Analysis and classification of heart sounds and murmurs based on the instantaneous energy and frequency estimations," in *Proceedings of the IEEE International Conference on Intelligent System and Technologies for the New Millennium (TENCON '00)*, vol. 2, pp. 130–134, Kuala Lumpur, Malaysia, September 2000.

[15] A. R. Abdullah, A. Z. Sha'ameri, and A. Jidin, "Classification of power quality signals using smooth-windowed Wigner-Ville distribution," in *Proceedings of the IEEE International Conference on Electrical Machines and System (ICEMS '10)*, pp. 1981–1985, Incheon, Korea, October 2010.